Author's post-print :A. Alonso-Estébanez, J. J. Del Coz Díaz, F. P. Álvarez Rabanal & P. Pascual-Muñoz (2017) Numerical simulation of bus aerodynamics on several classes of bridge decks, Engineering Applications of Computational Fluid Mechanics, 11:1, 435-449, DOI: 10.1080/19942060.2016.1201544

Numerical simulation of bus aerodynamics on several classes of bridge decks

A. Alonso-Estébanez [a,∗], J.J. del Coz Díaz[b], F.P. Álvarez Rabanal[b], P. Pascual-Muñoz[a]

[a] Department of Transport, Project and Process Technology, University of Cantabria, Av. Castros s/n, 39005 Santander, Spain.
[b] Department of Construction, GICONSIME Research Team, University of Oviedo, Departmental Building 7, 33204 Gijón, Spain.

Abstract

This paper is focused on improving traffic safety in bridge under crosswind conditions because adverse wind conditions increase the risk of traffic accidents. In this work, two ways in order to improve traffic safety are proposed to study. Vehicle stability can be improved on the one hand by means of wind fences installed on bridge deck and on the other hand by modifying design parameters of the infrastructure. Specifically, this study examines the influence of different parameters related to bridge deck configuration on the aerodynamic coefficients acting on a bus model under crosswind conditions. The aerodynamic coefficients related to: side force; lift force and rollover moment, were obtained for three classes of bridge deck (box, girder and board) by numerical simulation. The FLUENT code was used in order to solve Reynolds-averaged Navier–Stokes (RANS) equations along with the SST $k-\omega$ turbulence model. Two crash barriers located on the box bridge deck were replaced by an articulating wind fence model and then, the effect of angle between the wind fence and the horizontal plane on the bus aerodynamic was presented. The risk of having rollover accidents is slightly influenced by the bridge deck type for a yaw angle range between 75º and 120º. In order to study the effect of yaw angle on aerodynamic coefficients acting on bus, both the bus model and bridge model were simultaneously rotated. The minimum value of rollover coefficient was obtained for an angle 60º between the wind fence slope and the horizontal plane. The only geometry parameter of box bridge deck which significantly affects bus aerodynamics is the box height. The present research highlights: the usefulness of computational fluid dynamics codes for improving traffic safety, the performance of articulating wind fence, which geometry parameters of box deck have a significant influence on bus stability.

Keywords: Crosswind; Bridge decks; Heavy vehicle aerodynamics; Finite volume method (FVM); Computational fluid dynamics (CFD).

∗ Corresponding author. Tel.: +34-942-200894; fax: +34-942-201703.
E-mail address: alonsoea@unican.es. A. Alonso-Estébanez (Ph.D.).

1. Introduction

Wind conditions in locations such as bridges and viaducts may be especially negative for vehicle stability. Particularly, the control of high-sided vehicles requires more attention because they are more likely to undergo rollover or lane changing accidents (Baker & Reynolds, 1992 and Dorigatti et al., 2012). Nevertheless, in Cheung and Chan (2010), it is demonstrated that light-weight vehicles are also likely to suffer lack of comfort while driving on bridges under relatively low wind velocity. Nowadays, some authorities around the world opt for closing bridges when the wind velocity exceeds a limit value. In some cases this wind velocity limit is set based on previous experience instead of being the result of a quantitative procedure, which better guarantees user safety.

The interruption of traffic on some bridges may involve huge economic losses, especially if the bridges are associated with the local market logistics. Therefore, viaducts or bridges usually exposed to cross-wind conditions can be the cause of safety and economic issues. As a consequence, several research works have dealt with the outcome of crosswind on bridges (Wang, Xu, Zhu, Cao & Li, 2013 and Wang, Xu, Zhu & Li, 2014). Some of them have focused on the development of procedures to regulate traffic such as Cheung and Chan (2010) and Guo and Xu (2006), while other research studied wind fence efficiency (Rocchi, Rosa, Sabbioni, Sbrosi & Belloli, 2012 and Kozmar, Procino, Borsani & Bartoli, 2012). Improving knowledge about the aerodynamic behaviour of wind fences located on bridge decks is necessary, since many researchers have focused on the design of wind fences located on the ground where the wind conditions are different (Judd, Raupach & Finnigan, 1996 and Chen, Wang, Sun & Li, 2012).

Another aspect studied is the huge influence of wind conditions (wind velocity, approaching turbulence, wind direction, etc.) on vehicle stability. Kozmar *et al.* (2012) highlighted that high-sided vehicles suffer higher wind loads as the angle formed by the wind direction and the horizontal line in a vertical plane was increased. Charuvisit, Kimura and Fujimo (2004) indicated that an increase in wind velocity reduced the comfort during driving. In addition, the worst value of the horizontal angle formed by wind direction and the normal to bridge direction was 30º for the stability of vehicle. However, Bettle, Holloway and Benart (2003) particularized the most critical wind direction for the windward/leeward lane as 90º and 56.3º respectively. Another wind characteristic which should be considered when evaluating the risk of accident on roads is the presence of wind gusts because of their negative influence on vehicle stability (Kozmar, Butler & Kareem 2009).

Vehicles suffer huge instabilities under cross-wind conditions (Argentini, Ozkan, Rocchi, Rosa & Zasso, 2011 and Wang et al., 2014) at the towers on the bridges. In Charuvisit *et al.* (2004) the effect of tower geometry on vehicle stability was studied. The maximum yawing acceleration on the vehicle was higher for one of the tower models, so some modifications in the tower design could benefit traffic safety. Other part of bridges which can affects vehicle stability, is the bridge deck model`s geometry (Dorigatti et al., 2012 and Suzuki, Tanemoto & Maeda, 2003). In Dorigatti *et al.* (2012), the aerodynamic coefficients of three types of vehicles (van, truck and bus) were obtained for two bridge deck models, and the bus stability was sensitive to the different geometries. Suzuki *et al.* (2003) found out that an increase in the thickness of a bridge girder also causes the aerodynamic side force coefficient of vehicles to rise. Cheli, Corradi, Rocchi, Tomasini and Maestrini (2010) and Bettle *et al.* (2003) obtained the aerodynamic loads acting on vehicles located in the windward lane and the leeward lane. In both studies, the results indicated that aerodynamic loads were higher when the vehicles are travelling closer to the windward edge of the deck. Specifically, the rollover moment in the leeward lane was 30% lower than in the windward lane. To carry out these studies, the most frequently used techniques are (Bettle et al., 2003, Cheli, Corradi, Sabbioni & Tomasini, 2011 and Hibino, Shimomura & Tanifuji, 2010): numerical simulation (CFD), wind tunnel test and full scale experiments. In many cases the results from numerical simulations are contrasted with the other techniques (Sterling et al., 2010 and Sun, Zhang, Guo, Yang & Liu, 2014).

This study has been proposed to help competent authorities in traffic safety management on bridges under adverse crosswind conditions. As a consequence, the following objectives are established:

- Identify which type of bridge decks most adversely affects bus aerodynamics.
- Obtain the relationship between the angle of the wind fence slope and the aerodynamic coefficient acting on the bus model when it is located on a bridge.
- Determine whether it is possible to reduce the aerodynamic coefficients of bus by modifying the design parameters of a bridge deck.

To achieve these objectives, 3D CFD numerical simulations were carried out in order to study the stability of a 1:40 scale model bus located on a bridge under cross-wind conditions. During this study, the main difficulties were found when: setting the grid parameters, selecting one turbulence model between the options provided by FLUENT and proposing the most interesting study cases. In order to overcome these difficulties, on the one hand several numerical models with different grid sizes and turbulence models were solved and, on the other hand, investigations focused on the effect of crosswind conditions on traffic safety in bridge decks were studied in detail to propose interesting study cases (Wang et al., 2013; Wang et al., 2014 and Dorigatti et al., 2012).

In section 2, both the numerical setup and mathematical method required to solve the studied cases are defined. Then, in section 3, the procedure used both to select the turbulence model and to define the grid size setup is presented considering experimental data (Dorigatti et al., 2012). In section 4, the geometric parameters of a bridge deck with box are defined which were studied by using surface response methodology along with the Design of Experiment (DOE) technique. In section 5, results of bus aerodynamics and flow behavior around the bridge decks and an articulating wind fence are indicated and discussed. In the last section, the main conclusions from the results of this study are explained.

2. Numerical method

All numerical models were solved by using the CFD code, FLUENT-ANSYS. Next, the geometries for the bus and the bridge decks proposed to study are presented.

2.1. Bridge decks and aerodynamic loads

The influence of the bridge deck typology on vehicle stability was studied by obtaining the aerodynamic coefficients from the bus model. Among the types of bridge deck sections built nowadays, the following three were proposed for study: box, board, and girder (see Fig. 1). The aerodynamic coefficients acting on the bus located on the bridge decks were obtained for four yaw angle values: 75º, 90º, 105º and 120º. Detailed information about the dimensions of both the bus and box bridge deck (model scale 1:40) can be found in Dorigatti et al. (2012). This experimental study in wind tunnel was used to fit the numerical setup parameters and then this setup was applied to the other cases proposed to study. Four crash barriers 1250 mm high at full scale and porosity (ratio between open area and total area projected on the normal plane to wind direction) approximately 35%, were installed on the three types of bridge deck. These barriers are composed of two strips with a width of 406.25 mm and a gap between them of 218.75 mm in full scale. An additional model was built for the box bridge deck in which two of the crash barriers were replaced by solid and articulating wind fences (porosity 0%). The wind fence model was dived into two parts of equal length, but the upper part varied its slope angle with the road plane while the lower part was kept in vertical position (90º with the road plane) for all cases. Specifically, five values of slope angle, β, between 60º and 120º were studied. In vertical position, the articulating wind fence keeps the same height of crash barrier. Furthermore, the effect of the box deck design parameters (Fig 1 a) on the aerodynamic loads acting on the bus was studied by applying the response surface methodology.

On the other hand, the aerodynamic loads and moments acting on the bus obtained are side force (F_S), lift force (F_L) and rollover moment (M_R) (Fig. 2). The moments caused by side force and lift force were obtained by integrating the pressure about origin of reference system (point O in Fig. 2), due to wind force components acting in the x and y axes respectively. The rollover moment was calculated by adding the moments caused by side and lift forces. Then, these aerodynamic loads were become into non-dimensional coefficients using the following equations:

$$C_S = \frac{F_S}{\frac{1}{2}\rho U^2 A_S} \tag{1}$$

$$C_L = \frac{F_L}{\frac{1}{2}\rho U^2 A_S} \tag{2}$$

$$C_R = \frac{M_R}{\frac{1}{2}\rho U^2 A_S H} \tag{3}$$

where ρ is the density of the air, 1.18 kg/m^3; A_S is the side area of the bus, 27830 mm^2 (scale model); and H is the height of the bus, 110 mm (scale model) and U is the undisturbed wind speed measured 7 m upstream of the bridge deck section model.

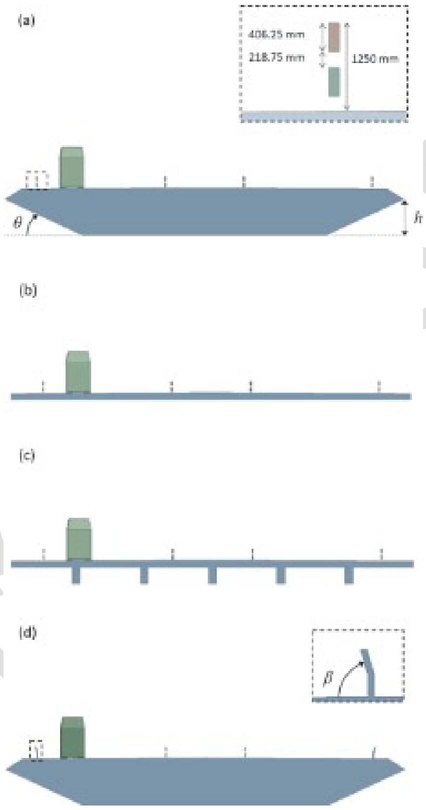

Fig 1 Configurations of bridge decks studied: (a) box, (b) board, (c) girder and (d) box with solid fence.

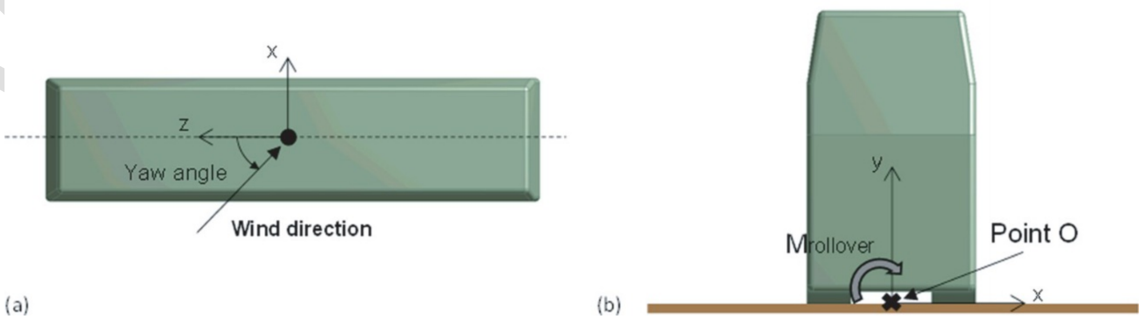

Fig 2 Sign convention for forces and moment and origin of coordinate reference system.

2.2. Mathematical approach

The lower region of the atmosphere where transport infrastructure are located is characterized by turbulent flows. Consequently, the Reynolds-averaged Navier-Stokes (RANS) equations in steady state along with a turbulence model were solved to predict the aerodynamic coefficients acting on the bus by using the finite volume method. In this work, a steady state analysis is applied instead of transient analysis because in order to achieve the objectives of study is not required. In addition, the computational cost and CPU time is quite higher for unsteady simulation as compared to the steady approach. For example, in turbomachinery applications as a rough estimation, Large Eddy Simulation (LES) would need around 5000 times the computational time of a steady analysis concerning RANS (Gourdain, Gicquel & Collado, 2012). The flow field around a vehicle is unsteady and very complex, including various time and length scales. Therefore, if the study requires high accuracy in the result obtained it would be necessary to carry out a transient analysis. However, if the goal is to predict which structural configuration influences more negatively the vehicle stability, as in the present study, the steady approach should be accurate enough. Nevertheless, to study the effect of using a steady approach instead of an unsteady one, the aerodynamic coefficients acting on the bus were obtained by both procedures for the box bridge deck (Section 4). The RANS equations govern the fluid movement through the three fundamental conservation principles: mass, momentum and energy. On the other hand, the turbulence models help to estimate the Reynolds stress and consequently, to close the equation system composed by the RANS equations. Among the potential turbulence model implemented in the CFD code, the bus aerodynamic coefficients were obtained for three of them: Spalart-Allmaras (Spalart & Allmaras, 1994), standard $k-\varepsilon$ (Launder & Spalding, 1974) and *SST* $k-\omega$ (Menter, 1994). The near wall region is solved by different methods according to the turbulence model applied. The Spalart-Allmaras model uses a formulation that blends automatically from a viscous sublayer formulation to a logarithmic formulation based on the value of y+. Therefore, this wall treatment can be used to solve the near wall region with independence of the refinement level of the grid. As for the standard $k-\varepsilon$ turbulence models, an enhanced wall treatment was chosen to solve near wall region instead of a standard wall function, because of the higher accuracy of this method to predict the flow behavior in the air regions close to walls. This approach combines a two-layer model with the so-called enhanced wall functions. If the near-wall mesh is fine enough to be able to resolve the viscous sublayer (y+ ≈ 1), a two-layer approach is applied, while if mesh is coarse, enhanced wall functions are used. The enhanced wall functions formulate the law of the wall as a single law for the entire wall region (viscous sublayer, buffer region and fully-turbulent outer region) by blending the linear (laminar) and logarithmic (turbulent) law-of-the-wall. This feature allows solving the near wall regions with different density of grids. The main difference between the standard $k-\varepsilon$ model and $SST\,k-\omega$ model regarding the near wall treatment applied, consists of the fact that the ω-equation can be solved through the viscous sublayer without the need for a two-layer approach that has to be used with the ε-equation. The results obtained for each turbulence model studied will be presented in Section 3. Detailed information on the RANS equations and the turbulence models equations can be found in FLUENT user manual.

In the finite volume method, the fluid domain is divided into a finite number of cells with nodal points. The shape and position of control volumes with respect to grid cells is defined according to a cell-centered scheme. Therefore, the control volumes are equal to the grid cell both in shape and position. These control volumes are delimited by the nodal point in the grid and the variables values are stored at centroids of the grid cells. The governing partial differential equations are integrated over the control volumes to evaluate the convective and viscous fluxes as well as the source term. Then, the equations in integral form are discretized to transform them into algebraic equations by applying quadrature formulae. These algebraic equations contain the values of variables and fluxes at the control volume faces which will be expressed in terms of the center values by interpolation scheme.

In the present study, a second-order upwind scheme was used for the moment equations and the turbulence quantities and, second order scheme for pressure equation during the spatial discretization. The variable gradients between the cell centroids were evaluated by the Least Squares Cell-Based method. The SIMPLE algorithm of Patankar and Spalding (1972) was used to solve pressure–velocity coupling. Finally, the algebraic equation system was solved by an iterative method.

2.3. Boundary conditions and grid

The three-dimensional domain, which contains the regions of air around both the bus and bridge deck models, has a cross section with the same dimensions that Wind Tunnel section of Polytechnic of Milano, 14 m x 4 m (Bocciolone, Cheli, Corradi, Muggiasca & Tomasini, 2008). The upstream and downstream distance between the bridge deck and the boundary surfaces (Fig. 3) exceeded the minimum values established under the European regulation EN 14067-6:2010. These distances are expressed as function of the obstacle height, H_{obs} (distance between the top surface of bus and the bottom surface of bridge deck). The numerical simulation was carried out with still bus model without reproducing the relative movement between bus and bridge deck because computational cost is greater and, vehicle motion has no significant influence on the force coefficients according to Bocciolone et al. (2008). In order to obtain the aerodynamic coefficients for each value of the yaw angles studied when the bus model is located on the three types of bridge decks, the bus and bridge deck were rotated together as it is shown in Fig. 4.

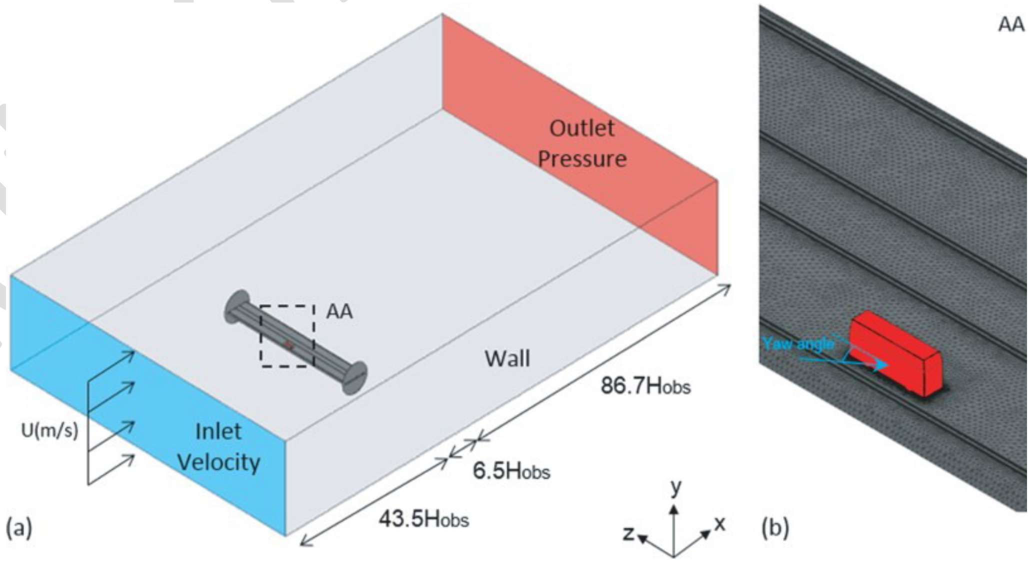

Fig 3 (a) Geometrical model of the numerical domain and boundary conditions. (b) Bus model on the bridge deck for the numerical simulation.

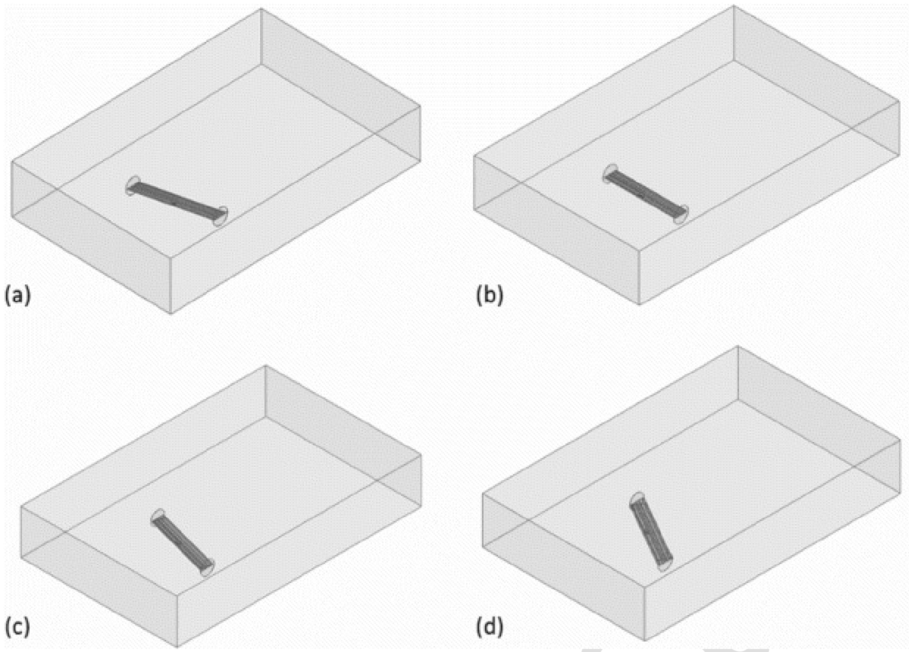

Fig 4 Yaw angle positions studied by numerical simulation: (a) 75º; (b) 90º; (c) 105º; (d) 120º.

The domain was broken up in two sub domains (far domain and near domain in Fig. 5) to build a finer grid in the air region close to the bus model where strong gradients of the flow variables originate. In the near domain two types of cells were used, specifically wedge cells for the air regions near bus surface by applying a inflation control and tetrahedral cells for the other region of domain, while in the far domain was only used tetrahedral cells. The wedge grid performs well in solving the near-wall region problem, which can be subdivided into three layers: viscous sublayer; buffer layer; and log-law region. A total of ten inflated layers of wedge with a growth rate of 1.1 make up the wedge grid, the thickness of the first layer being set to obtain an y^+ not exceeding 1. The variable y^+ is the dimensionless distance from the wall, related to the distance from the wall y, shear velocity u_τ (value of the friction velocity obtained from the experimental wind profile) and kinematic viscosity ν as follows:

$$y^+ = \frac{u_\tau \cdot y}{\nu} \tag{4}$$

A finer grid was built for both the air region close to curved surface and small gap of air between walls by using curvature and proximity controls. In the next section, the boundary condition setup is detailed (Tu, 2013, Moaveni, 2014 and Madenci & Guven, 2015):

- **Inlet Velocity:** A uniform profile of 13.5 m/s was defined for the flow velocity, *U* (see Fig 3). $V, W = 0$ (components of wind velocity in *y* and *z* directions are zero). The turbulent length scale, *l* and turbulence intensity, *I* are ~ 30 m (full scale value) and 6% respectively according to experimental conditions (Dorigatti et al., 2012). The flow is incompressible and subsonic (Versteeg & Malalasekera, 2007):

$$\mathrm{Ma} = \frac{U}{c} = \frac{13.5\ \ m/s}{340\ \ m/s} = 0.04 \ll 0.3 \Rightarrow \nabla \cdot \vec{u} = 0 \qquad (5)$$

- **Outlet Pressure:** Relative pressure *p* = 0. The normal gradients of all variables were set equal to zero (Neumann boundary condition). Under back flow conditions, the average turbulence intensity, *I*, and turbulent length scale, *l*, were assigned the inlet boundary condition values.
- **Solid walls:** A non-slip condition (*U*,*V*,*W*=0) was adopted on the solid surfaces of the domain. The roughness height was set to a null value, therefore the boundary surface behaves as a smooth surface.

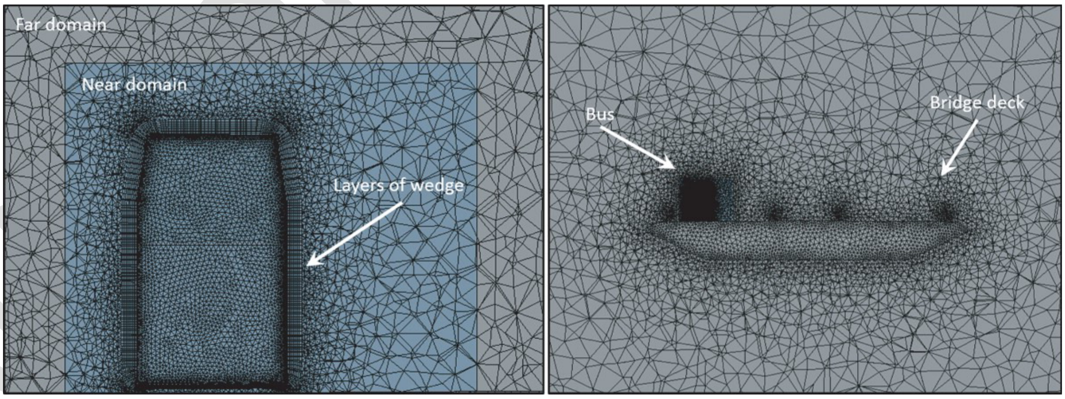

Fig 5 View of the grid employed for the different regions of the domain.

3. Grid size and turbulence closure model

The spatial discretization error can be decreased by diminishing the cell size but a smaller cell size increases the total number of cells in the grid and, in consequence the computational cost.

Therefore, a grid size independence study was carried out to avoid wasting computational power. In particular, the aerodynamic coefficients acting on the bus located on the box bridge deck with a yaw angle of 90º were obtained for four grid sizes: 13.4; 16.2; 19.1 and 22.8 million. The distribution of elements by types for the grid size built is exhibited in Table 1. In the sensitivity analysis of grid size, the $SST\,k-\omega$ model was used instead of the Spalart-Allmaras and standard $k-\varepsilon$ models. This is due to the harder requirements required by this model on the mesh refinement as compared to the others.

Table 1. Distribution of elements for several grid sizes.

Grid size (million)	Tetrahedrons (%)	Wedges (%)
13.4	94.02	5.98
16.2	95.05	4.95
19.1	89.7	10.3
22.8	96.48	3.52

The different levels of refinement were obtained by applying a size control function on the near domain, which is the air region where the variable gradients are stronger and a smaller cell size is likely required (Fig 6).

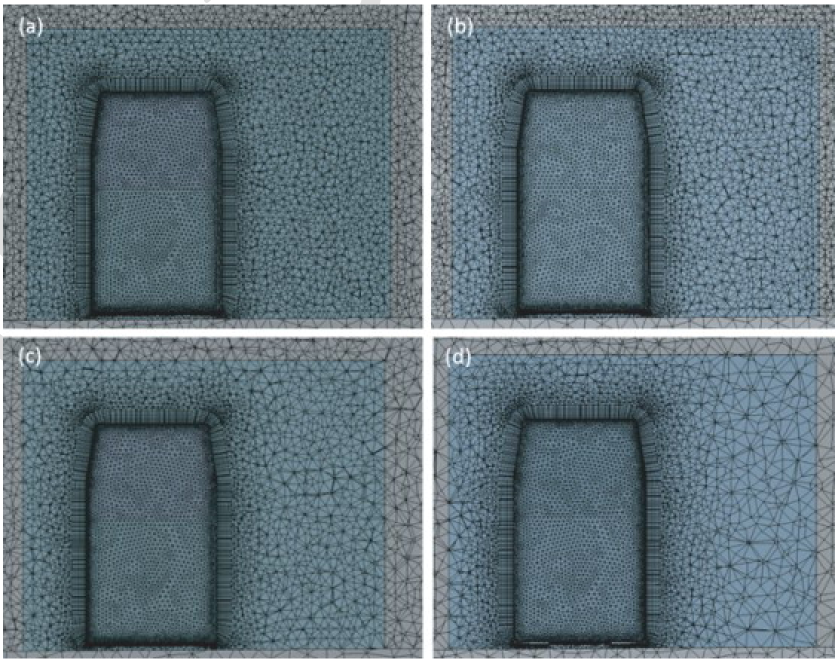

Fig 6 Grid in the region where the refinement was applied for the following grid sizes: (a) 22.8; (b) 19.1; (c) 16.2 and (d) 13.4 million.

The results indicate that the aerodynamic coefficients acting on the bus are quite independent of the grid size for the studied range of cells number (Fig. 7). Thus, the grid setup defined for 13.4 million cells was applied to the other numerical simulations.

The grid size varies with the yaw angle studied for the three types of bridge decks. Specifically, the maximum variation of grid size with the yaw angle taking as the reference the grid size value for 90º yaw angle in each bridge deck type and, keeping the same grid setup, is shown in the Table 2.

Table 2. Yaw angle where the maximum variation of grid size with respect to 90º of yaw angle was obtained for each bridge deck.

Bridge deck	Yaw angle (º)	Maximum variation of grid size (million)
Box	75	1
Board	120	0.4
Girder	120	1.9

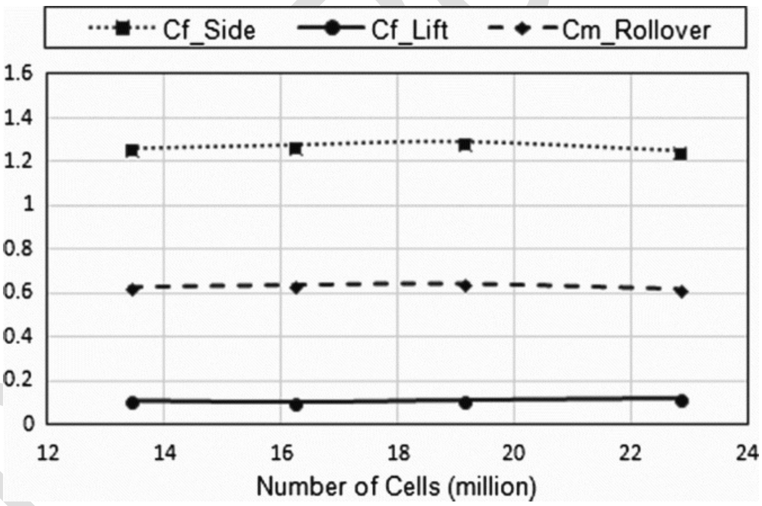

Fig 7 Influence of grid size on aerodynamic coefficients of bus for box bridge deck.

Then, the relative errors between the aerodynamic coefficients obtained by numerical modelling with three turbulence models (Spalart-Allmaras, standard $k-\varepsilon$ and $SST\,k-\omega$) and, by experimental test (Dorigatti et al., 2012) were determined to select the turbulence model.

The lowest relative error in the three coefficients was obtained with the $SST\,k-\omega$ model (see Table 3); therefore, this model was finally used in the other scenarios. The lift coefficient exhibits the highest relative error, this could be because the components, which were used to link the balance and the bus model in the experimental test, were not defined in the numerical simulation since these geometric details are not indicated in Dorigatti et al. (2012). Specifically, the experimental value of lift coefficient is lower than the value obtained by numerical model, due to the smaller air gap between the bus model and the road surface as consequence of components used to link the bus model and the balance in the experimental test. This smaller gap causes higher values of velocity and lower values of static pressure in the air flow under the bus and consequently, the lift force diminishes as compared with numerical values. On the other hand, these components are actually supposed to modify the air flow through the gap between the bus and road surface with respect to real conditions.

The results of numerical models can be considered accurate enough to reach the objective set for this study, due to the following reasons: the weight of lift coefficient on the rollover coefficient is rather softer than the side coefficient; the lift force values are quite lower than the side force and as consequence when the difference between numerical and experimental values are expressed in terms of relative error, the error relative of lift coefficients is quiet higher than the others; and finally the relative error of the side coefficient is low enough to rely on this value.

One of the main characteristic of $SST\,k-\omega$ model is its good performance in order to solve low Reynolds flows as those present in the near wall regions (ANSYS Inc. 2011 and Tu, 2013). Many authors recommend that the $SST\,k-\omega$ model should replace the standard $k-\varepsilon$ model as the first choice (Andersson et al., 2011).

Table 3. Relative error for the aerodynamic coefficients as a function of turbulence model in the box bridge deck.

Turbulence Model	Aerodynamic Coefficients		
	Cf_Side	Cf_Lift	Cm_Rollover
K-ϵ	0.18	7.00	0.12
SST k-ω	0.01	3.75	0.05
Spalart-Allmaras	0.25	6.50	0.23

Author's post-print :A. Alonso-Estébanez, J. J. Del Coz Díaz, F. P. Álvarez Rabanal & P. Pascual-Muñoz (2017) Numerical simulation of bus aerodynamics on several classes of bridge decks, Engineering Applications of Computational Fluid Mechanics, 11:1, 435-449, DOI: 10.1080/19942060.2016.1201544

4. Comparison between unsteady and steady aerodynamic coefficients

An unsteady numerical simulation with the $SST\,k-\omega$ model was carried out prior to the use of the steady approach for the proposed cases. Thus, the box bridge deck was used to calculate the aerodynamic coefficients of bus by applying both a steady approach as unsteady. The nondimensional time step was set as $\Delta t^* = \Delta t \cdot U_\infty / H = 0.097$ (H is the height of bus as in Ai & Mak, (2015)), keeping a CFL number (Courant–Friedrichs–Lewy) below 1 in the most of the cells of regions with flow detaching. The simulations were run for a time of $2712\,\Delta t^*$, the time required by the air flow to cover 3 times the domain. The first $556\,\Delta t^*$ were not considered to calculate the average values of aerodynamic coefficient because the values were not stable. Fig 8 shows the relationships between the average values of the aerodynamic coefficients and the yaw angle for the two numerical approaches (steady and unsteady) and the experimental test (Dorigatti et al. (2012)). The unsteady analysis exhibits values of aerodynamic coefficients closer to experimental measurements, however, the variations of the aerodynamic coefficients with the yaw angle are quiet similar by applying both approaches. Therefore, the steady approach will allow the obtention of accurate enough trends as for reaching the objectives of this study.

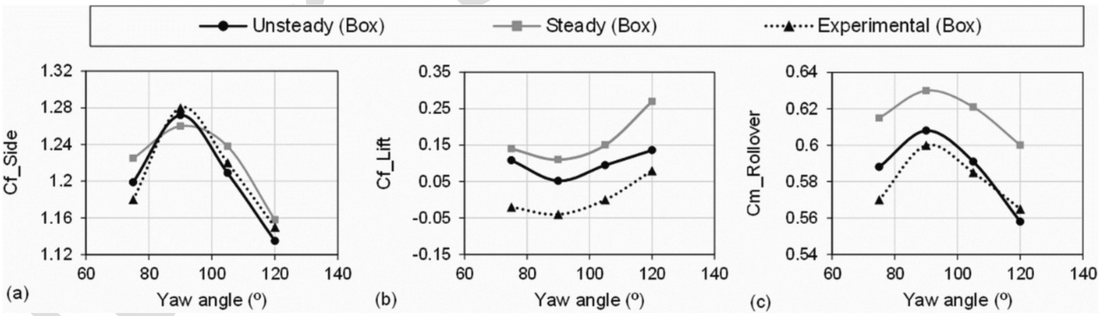

Fig 8 Comparison between the aerodynamic coefficients –(a) side force, (b) lift force and (c) rollover moment– obtained by steady and unsteady approaches and experimental test (Dorigatti et al. (2012)).

5. DOE methodology

In order to study the effect of the box deck design parameters on the aerodynamic loads acting on the bus, a sensitivity analysis and a design of experiments (DOE) analysis were carried out. In this sense, the result from DOE analysis enables the optimization of the box deck configuration. A central composite design (CCD) was chosen to determine the number of cases required to perform the study as a part of DOE methodology (Myers, Montgomery & Anderson-Cook, 2009 and Del Coz Díaz, Serrano López, López-Colina & Álvarez Rabanal, 2012). Then, the output and input variables were selected throughout the range of study in the case of the latter. Each combination of input variables requires calculating the output variables by means of a new volume finite analysis. A response surface model is obtained according to the second order polynomial regression model set and the results from the DOE study. The response surface is an explicit approximation function, which expresses the output data as a function of input data by the fitting algorithm indicated in the DOE methodology.

As a part of the DOE procedure the higher-order derivatives are evaluated from the results generated for each design point, the order of the derivatives indicates the order of the approximation expressions. The second-order model applied in the present work considering two input variables can be written as follow:

$$Y = \lambda_0 + \lambda_1 x_1 + \lambda_2 x_2 + \lambda_{11} x_1^2 + \lambda_{22} x_2^2 + \lambda_{12} x_1 x_2 + error \tag{6}$$

where, Y is the predicted response variable, the Xs are the factors or input variables. There are 1 two-way interaction terms according to $p(p-1)/2 = 2\times 1/2 = 1$, two quadratic terms and two linear terms. The regression coefficients, λs were calculated by the ordinary least squares (OLS) procedure, where the OSL estimator can be written as:

$$\vec{\lambda}_{OLS} = \left(\vec{X}^T \vec{X}\right)^{-1} \vec{X}^T \vec{Y} \tag{7}$$

where $\vec{X}$ is the extended designed matrix for the input variables including the coded levels and $\vec{Y}$ is a column vector of output variable values obtained for the specify points in the DOE. The input variables over their variation range (maximum, minimum and current value) and the output variables are as follows:

- ***Input variables*** (see Fig. 1): the height of deck box, h and angle of deck box, θ. On the one hand, the height of deck box is varied from 25 mm to 92.5 mm (in full scale from 1 m to 3.7 m), the starting design value being of 58.75 mm (2.35 m in full scale). On the other hand, the range of deck box angle is from 15º to 45º, with a starting design value of 30º.

- ***Output parameters***: the aerodynamic coefficients associated with side force, lift force and rollover moment.

6. Result and discussion

In this section, the influence of both the bridge deck configuration and of wind fence slope on aerodynamic loads which contribute to the rollover accident under crosswind conditions, is shown and discussed.

6.1. Bridge deck type effect

In order to study the effect of the bridge deck type on the stability of a bus model, the aerodynamic coefficients of bus were obtained in three types of bridge deck section, as it was indicated in Section 2.1. Fig. 9 illustrates the aerodynamic coefficients acting on the bus located on the three bridge decks considered for four yaw angle values: 75º, 90º, 105º and 120º. In order to obtain the aerodynamic coefficients for each value of yaw angle, the bus and the bridge deck were rotated together. While the side and the rollover coefficients approach the highest values for a yaw angle of 90º, the lift coefficient approach the lowest values. The side and the rollover coefficients show a similar trend with respect to the yaw angle due to the stronger influence above the rollover moment by the side force than the lift force. However, the lift coefficient exhibits an opposing behavior to the other coefficients as in Dorigatti et al. (2012). The side and rollover coefficients diminish when the yaw angle moves away from the perpendicular to the traffic direction and the lift coefficient increases. Moreover, the differences between aerodynamic coefficients for the three type of bridge decks are quite small but, the board type seems to influence more negatively the bus stability than the other decks for most of the yaw angle values. A sample of numerical results relative to static pressure and wind velocity in the air region around of bus for a yaw angle of 90º, is illustrated in Fig. 10. These results indicate that there are not great differences between the bridge decks with respect to the air flow velocity around the bus, as Fig. 10 shows. However, it is interesting to stress that the bus stability could be improved if the bridge deck model caused a higher perturbation on the air flow hitting on the bus. The stronger gradients of pressure and velocity at the air region below the bridge decks (Fig. 10) are caused by the girder and box types, and these are the bridge decks where higher values of rollover coefficient are obtained.

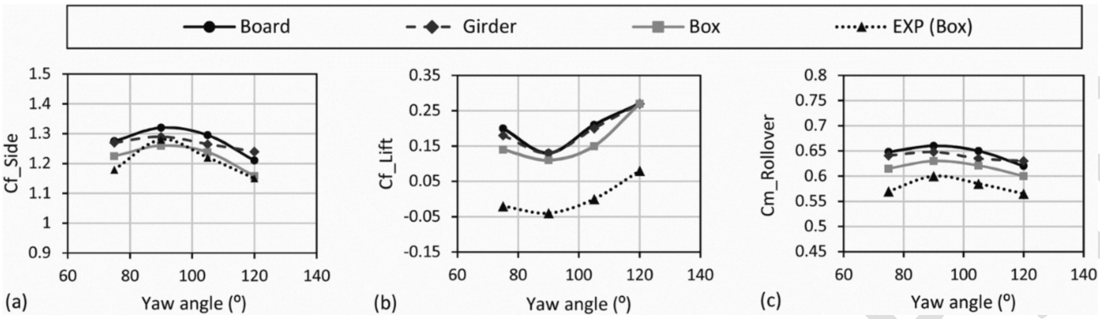

Fig 9 Relationships between the aerodynamic coefficients, obtained by CFD code and Dorigatti et al. (2012), and the yaw angle for different bridge decks. (a) Side force; (b) Lift force; (c) Rollover moment.

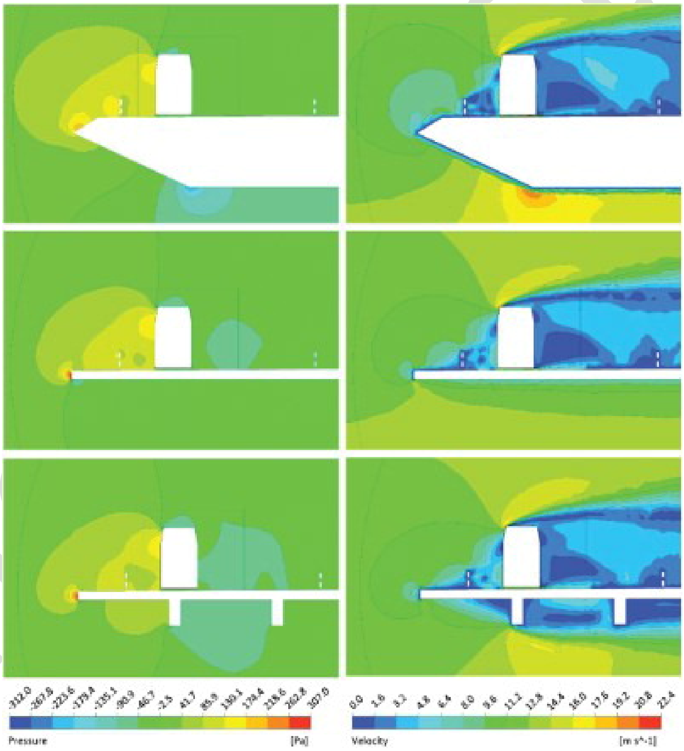

Fig 10 Pressure and wind velocity contours calculated for the three types of bridge deck with a yaw angle of 90º.

6.2. Influence of wind fence slope

In this section, the relationships between the wind fence slope (β angle) and the aerodynamic coefficients of the bus are studied under crosswind conditions (yaw angle of 90º). The most important parameter with respect to cross-wind stability is the rollover moment coefficient (Schober, Weise, Orellano, Deeg & Wetzel, 2010), therefore the wind fence performance was

Author's post-print :A. Alonso-Estébanez, J. J. Del Coz Díaz, F. P. Álvarez Rabanal & P. Pascual-Muñoz (2017) Numerical simulation of bus aerodynamics on several classes of bridge decks, Engineering Applications of Computational Fluid Mechanics, 11:1, 435-449, DOI: 10.1080/19942060.2016.1201544

evaluated through the reduction of this coefficient. Similar behaviour is exhibited in the side force coefficient and the rollover moment coefficient versus the wind fence slopes (Fig. 11), where two regions can be distinguished. In the first region, both coefficients decrease from a wind fence slope of 15º to 60º, where the minimum values are reached and keep quite constant until 75º, where coefficients begin to increase. The lift coefficient exhibits an opposite trend with respect to the rollover and side coefficients where the maximum value of lift coefficient is approached for a wind fence slope of 75º (Fig. 11). Among the slope angles of wind fence studied, 60º highlights as the position where the minimum value of rollover coefficient is obtained. For this slope angle value, a lower number of streamlines hit on the top zone of the windward surface of the bus in comparison with other values of wind fence slope, which result in a reduction of the rollover coefficient of the bus (Fig. 12). Specifically, this articulating wind fence reduces the rollover coefficient in relation to the crash barrier by a maximum value of 22% (wind fence slope angle of 60º). While the side coefficient of bus was higher when the crash barrier were installed, the lift coefficient was lower in comparison with the case of articulating wind fence. This difference in the lift coefficient is due in part to a lower air flow through the gap between the bus and the road for the articulating wind fence and, in consequence, the pressure is higher in the air region under the bus, what rises the difference of pressure between the top and underneath surfaces of bus.

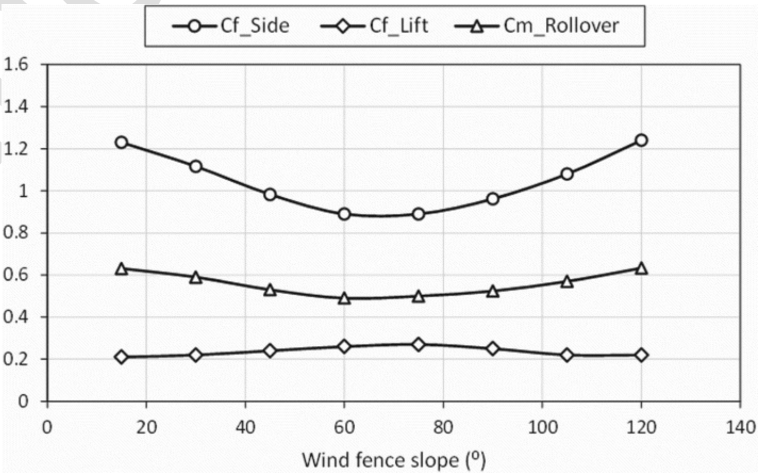

Fig 11 Relationship between aerodynamic coefficients of bus and wind fence slope for the box deck under cross wind conditions.

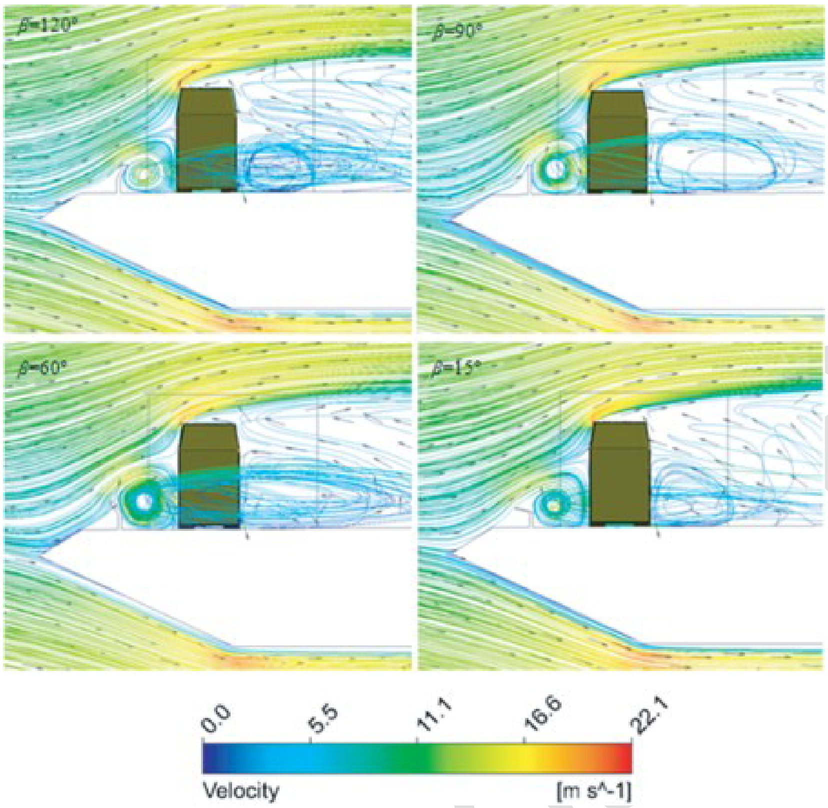

Fig 12 Streamlines of velocity field around of bus for four values of wind fence slope angle, β.

6.3. Configuration of box bridge deck

In this section, the influence of two geometrical parameters of box bridge deck on bus aerodynamics was studied by solving 9 numerical models. A converged solution was reached when the following requirements were fulfilled: the scaled residuals of all the variables were less than $1 \cdot 10^{-5}$, the net flux imbalance was less than 1% of the smallest flux through the domain boundary and the monitored aerodynamic coefficient keep constant in 4 significant figures (ANSYS Inc. 2011). In order to carry out the simulations, a server with a CPU Intel Xeon 5630 @ 2.53 GHz (8 processors), 64 GB RAM memory, 4 TB hard disk were used and worked under the Windows server 2003 operating system was used. The geometry input parameters described in Section 4 were coded in three values (-1, 0, 1) by applying this expression (Montgomery, 2013):

$$x_{coded} = \frac{x - \left(x_{low} + x_{high}\right)/2}{\left(x_{low} - x_{high}\right)/2} \tag{8}$$

The response surface models fitted with the results obtained after solving the cases proposed by the design of experiment are plotted in Fig. 13. These graphs show the maximum variation of aerodynamic coefficients of the bus caused by the effect of deck box height and deck box angle within a predetermined range of values. The adjusted coefficients of determination, R^2_{adj}, related to the response surface models are: 0.79 for the lift coefficient, 0.76 for the side coefficient and 0.69 for the rollover coefficient. Among the cases solved, the best configuration of box deck will be the one for which the minimum coefficient of rollover is reached. Specifically, a minimum value of 0.628 for the rollover coefficient is obtained for a box angle of 45º (+1 coded value) and a height of 92.5 mm (+1 coded value) as it is shown in the Fig 13. However, the influence of this parameters on both the rollover coefficient and side coefficient is quiet modest because the response variation with respect to the average value is below 5%. In the case of lift coefficient, it reaches a maximum variation of 16% but its influence on the rollover coefficient is quite smaller than the side coefficient.

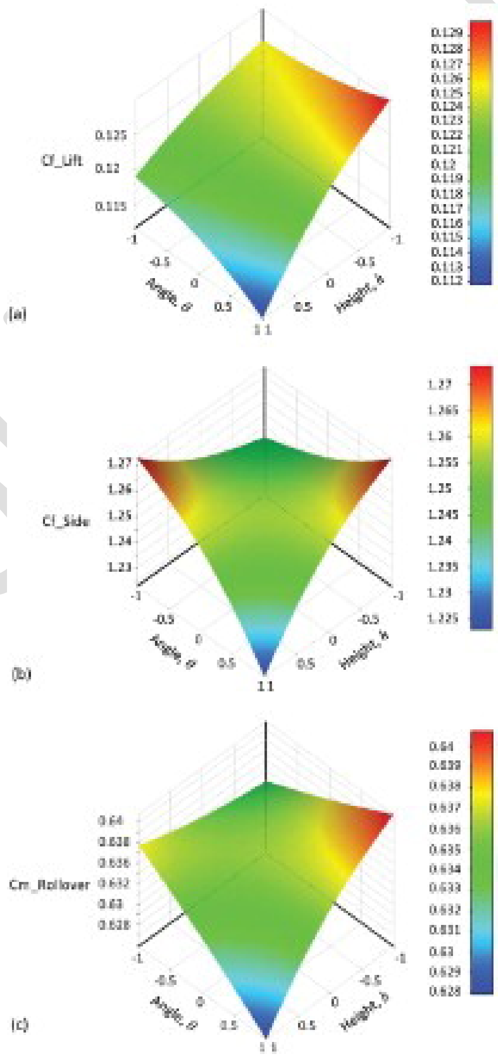

Fig 13 Response surfaces relating the geometrical parameters of a box deck (box angle and box height) with the following aerodynamic coefficients: lift force (a), side force (b) and rollover moment (c).

Author's post-print :A. Alonso-Estébanez, J. J. Del Coz Díaz, F. P. Álvarez Rabanal & P. Pascual-Muñoz (2017) Numerical simulation of bus aerodynamics on several classes of bridge decks, Engineering Applications of Computational Fluid Mechanics, 11:1, 435-449, DOI: 10.1080/19942060.2016.1201544

In addition, a sensitivity study was carried out for independent assessment of this geometrical parameter on the aerodynamic coefficient acting on the bus. The results indicate that the height of box significantly influences both the rollover coefficient and the lift coefficient while, the angle of box is not correlated with any aerodynamic coefficient (Fig. 14). The effect of height parameter above the rollover coefficient is due to the negative value of sensitivity between this parameter and the lift coefficient, because the side coefficient is not affected by the height of box. To sum up, the risk of rollover accident does not strongly depends on this geometry parameters of the box deck.

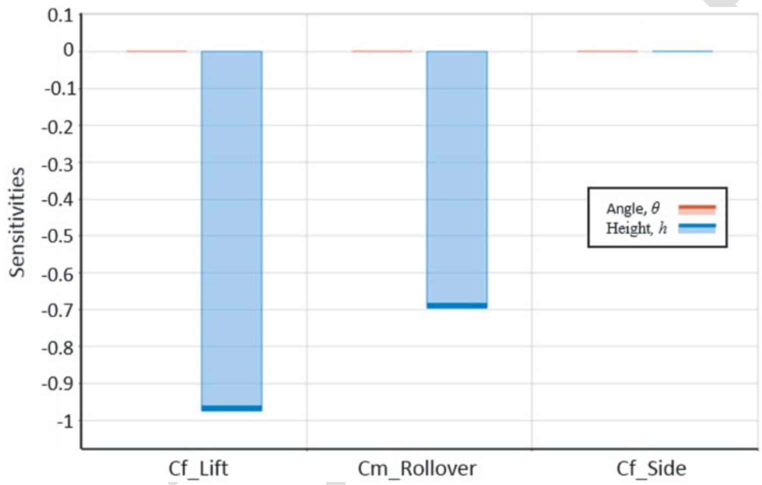

Fig 14 Global sensitivity values between the aerodynamic coefficients of the bus and the geometrical parameters of a box deck.

7. Conclusions

In this work, a methodology is developed to help distinguish scenarios on roads where crosswind conditions are more negative for traffic safety. The competent authorities will be able to use this information to decide, with more precise criteria, on issues such as: in which infrastructures it is most necessary to install a wind fence or when traffic must be closed on bridges due to strong crosswind. In addition, a new approach which consists in improving the traffic safety by modifying the structural configuration of bridge decks, was studied.

The main remarks from the quantitative results can be summarized as follows:

- Of the three types of bridge deck tested, the board type slightly influences more negatively bus stability than the other decks in the yaw angle range studied (75º - 120º).
- The effect of wind fence slope angle on the aerodynamic coefficients of the bus was studied and, the results exhibits that the minimum value of rollover moment coefficient was obtained for an angle of 60º with respect to the horizontal plane.
- The articulating wind fence reveals as a better option to protect the vehicles against cross wind conditions than the crash barriers. Specifically, this wind fence model reduces the rollover coefficient in relation to the crash barrier by a maximum value of 22%.
- The rollover coefficient acting on the bus exhibits variations below 5% for the two geometry parameters of box bridge deck studied; therefore, it can be stated that the risk of having rollover accidents does not strongly depend on these parameters.
- As regards numerical setup, the best fit to experimental data was obtained by using the SST $k-\omega$ turbulence model.
- The finite volume method has proved to be a powerful tool for solving the Reynolds averaged Navier–Stokes (RANS) equations along with the SST $k-\omega$ turbulence model.
- In the case of the box bridge deck case, the unsteady approach has shown to be more accurate than the steady approach. However, the trends in the result graphs are quiet similar for both approaches.
- In order to carry out a more detailed study of the unsteady behavior of the fluids around the bus, it might be interesting to apply other more accurate approaches with higher computational cost such as Large Eddy Simulation (LES), Detached Eddy Simulation (DES) or Scale Adaptive Simulation (SAS).

References

Ai, Z.T, & Mak, C.M. (2015). Large-eddy Simulation of flow and dispersion around an isolated building: Analysis of influencing factors. *Computer and Fluids,* 118, 89-100. DOI: 10.1016/j.compfluid.2015.06.006

Andersson, B., Andersson, R., Hakansson, L., Mortensen, M., Rahman, S., & Berend V.W. (2011). *Computational fluid dynamics for engineers*. New York, USA. Cambridge University Press.

Argentini, T., Ozkan, E., Rocchi, D., Rosa, L., & Zasso, A. (2011). Cross-wind effects on a vehicle crossing the wake of a bridge pylon. *Journal of Wind Engineering and Industrial Aerodynamics,* 99, 734-740. **DOI:** 10.1016/j.jweia.2011.01.021.

ANSYS Inc. (2011). *Fluent Manual Release 15.0.* Canonsburg, USA. PA.

Baker, C.J., & Reynolds, S. (1992). Wind-induced accidents of road vehicles. *Accident Analysis and Prevention,* 24, 559-575. **DOI:** 10.1016/0001-4575(92)90009-8.

Bettle, J., Holloway, A.G.L., & Venart, J.E.S. (2003). A computational study of the aerodynamic forces acting on a tractor-trailer vehicle on a bridge in cross-wind. *Journal of Wind Engineering and Industrial Aerodynamics,* 91, 573-592. **DOI:** 10.1016/S0167-6105(02)00461-0.

Bocciolone, M., Cheli, F., Corradi, R., Muggiasca, S., & Tomasini, G. (2008). Crosswind action on rail vehicles: Wind tunnel experimental analyses. *Journal of Wind Engineering and Industrial Aerodynamics,* 96, 584-610. **DOI:** 10.1016/j.jweia.2008.02.030.

Charuvisit, S., Kimura, K., & Fujino, Y. (2004). Effects of wind barrier on a vehicle passing in the wake of a bridge tower in cross wind and its response. *Journal of Wind Engineering and Industrial Aerodynamics,* 92, 609-639. **DOI:** 10.1016/j.jweia.2004.03.006.

Cheli, F., Corradi, R., Rocchi, D., Tomasini, G., & Maestrini, E. (2010). Wind tunnel tests on train scale models to investigate the effect of infrastructure scenario. *Journal of Wind Engineering and Industrial Aerodynamics,* 98, 353-362. **DOI:** 10.1016/j.jweia.2010.01.001.

Cheli, F., Corradi, R., Sabbioni, E., & Tomasini, G. (2011). Wind tunnel tests on heavy road vehicles: Cross wind induced loads-Part 1. *Journal of Wind Engineering and Industrial Aerodynamics,* 99, 1000-1010. **DOI:** 10.1016/j.jweia.2011.07.009.

Chen, G., Wang, W., Sun, C., & Li, J. (2012). 3D numerical simulation of wind flow behind a new porous fence. *Powder Technology,* 230, 118-126. **DOI:** 10.1016/j.powtec.2012.07.017.

Cheung, M.M.S., & Chan, B.Y.B. (2010). Operational requirements for long-span bridges under strong wind events. *Journal of Bridge Engineering,* 15, 131-143. **DOI:** 10.1061/(ASCE)BE.1943-5592.0000044

Dorigatti, F., Sterling, M., Rocchi, D., Belloli, M., Quinn, A.D., Baker, C.J., & Ozkan, E. (2012). Wind tunnel measurements of crosswind loads on high sided vehicles over long span bridges. *Journal of Wind Engineering and Industrial Aerodynamics,* 107-108, 214-224. **DOI:** 10.1016/j.jweia.2012.04.017.

Del Coz Díaz, J.J., Serrano López, M.A., López-Colina Pérez, C., & Álvarez Rabanal, F.P. (2012). Effect of the vent hole geometry and welding on the static strength of galvanized RHS K-joints by FEM and DOE. *Engineering Structures,* 41, 218-233. **DOI:** 10.1016/j.engstruct.2012.03.050.

EN 14067-6:2010. European Standard. Railway applications - Aerodynamics - Part 6: Requirements and test procedures for cross wind assessment. CEN, 2010.

Gourdain. N., Gicquel, L.Y.M., & Collado, E. (2012). Comparison of RANS and LES for prediction of wall heat transfer in a highly loaded turbine guide vane. J Propulsion Power, 28, 423–433. **DOI:** 10.2514/1.B34314.

Guo, W.H., & Xu, Y.L. (2006). Safety analysis of moving road vehicles on a long bridge under crosswind. *Journal of Engineering Mechanics,* 132, 438-446. **DOI:** 10.1061/(ASCE)0733-9399(2006)132:4(438).

Hibino, Y., Shimomura, T., & Tanifuji, K. (2010). Full-Scale Experiment on the Behavior of a Railway Vehicle being subjected to Lateral Force. *Journal of Mechanical Systems for Transportation and Logistics,* 3, 35-43. DOI: 10.1299/jmtl.3.35.

Judd, M.J., Raupach, M.R., & Finnigan, J.J. (1996). A wind tunnel study of turbulent flow around single and multiple windbreaks, part I: Velocity fields. *Boundary-Layer Meteorology,* 80, 127-165.

Kozmar, H., Butler, K., & Kareem, A. (2009, November). *Aerodynamic loads on a vehicle exposed to cross-wind gusts: An experimental study*. Paper presented in 7th Asia-Pacific Conference on Wind Engineering, APCWE-VII, Taipei, Taiwan.

Kozmar, H., Procino, L., Borsani, A., & Bartoli, G. (2012). Sheltering efficiency of wind barriers on bridges. *Journal of Wind Engineering and Industrial Aerodynamics,* 107-108, 274-284. **DOI:** 10.1016/j.jweia.2012.04.027.

Launder, B.E., & Spalding, D.B. (1974). The numerical computation of turbulent flows. *Computer Methods in Applied Mechanics and Engineering,* 3, 269-289. **DOI:** 10.1016/0045-7825(74)90029-2.

Madenci, E., & Guven, I. (2015). *The Finite Element Method and Applications in Engineering Using ANSYS*. New York. Springer.

Menter, F.R. (1994). Two-equation eddy-viscosity turbulence models for engineering applications. *AIAA Journal,* 32, 1598-1605.

Moaveni, S. (2014). *Finite Element Analysis: Theory and Application with ANSYS*. New York. Prentice Hall.

Montgomery, D.C. (2013). *Design and Analysis of Experiments* (8th edition). North Carolina, USA. John Wiley & Sons.

Myers, R.H., Montgomery, D.C., & Anderson-Cook, C.M. (2009). *Response Surface Methodology: Process and Product Optimization Using Designed Experiments*. New York. John Wiley & Sons.

Patankar, S.V., & Spalding, D.B. (1972). A calculation procedure for heat, mass and momentum transfer in three-dimensional parabolic flows. *International Journal of Heat and Mass Transfer,* 15, 1787-1806. **DOI:** 10.1016/0017-9310(72)90054-3.

Rocchi, D., Rosa, L., Sabbioni, E., Sbrosi, M., & Belloli, M. (2012). A numerical-experimental methodology for simulating the aerodynamic forces acting on a moving vehicle passing through the wake of a bridge tower under cross wind. *Journal of Wind Engineering and Industrial Aerodynamics,* 104-106, 256-265. **DOI:** 10.1016/j.jweia.2012.03.012.

Schober, M., Weise, M., Orellano, A., Deeg, P., & Wetzel, W. (2010). Wind tunnel investigation of an ICE 3 endcar on three standard ground scenarios. *Journal of Wind Engineering and Industrial Aerodynamics,* 98, 345-352. **DOI:** 10.1016/j.jweia.2009.12.004.

Spalart, P.R., & Allmaras, S.R. (1994). One-equation turbulence model for aerodynamic flows. *Recherche Aerospatiale,* 5-21.

Sterling, M., Quinn, A.D., Hargreaves, D.M., Cheli, F., Sabbioni, E., Tomasini, G., Delaunay, D., Baker, C.J., & Morvan, H. (2010). A comparison of different methods to evaluate the wind induced forces on a high sided lorry. *Journal of Wind Engineering and Industrial Aerodynamics,* 98, 10-20. **DOI:** 10.1016/j.jweia.2009.08.008.

Suzuki, M., Tanemoto, K., & Maeda, T. (2003). Aerodynamic characteristics of train/vehicles under cross winds. *Journal of Wind Engineering and Industrial Aerodynamics*, 91, 209-218. **DOI:** 10.1016/S0167-6105(02)00346-X.

Tu, J. (2013). *Computational fluid dynamics*. Oxford, UK. Butterworth-Heinemann.

Versteeg, H.K., & Malalasekera, W. (2007). *An Introduction to Computational Fluid Dynamics: The Finite Volume Method*. England. Pearson Education.

Wang, B., Xu, Y.L., Zhu, L.D., Cao, S.Y., & Li, Y.L (2013). Determination of aerodynamic forces on stationary/moving vehicle-bridge deck system under crosswinds using computational fluid dynamics. *Engineering Applications of Computational Fluid Mechanics*, 7, 355-368.

Wang, B, Xu, Y.L., Zhu, L.D., & Li, Y.L (2014). Crosswind Effect Studies on Road Vehicle Passing by Bridge Tower using Computational Fluid Dynamics. *Engineering Applications of Computational Fluid Mechanics*, 8, 330-344.

Sun, Z., Zhang, Y., Guo, D., Yang, G., & Liu, Y. (2014). Research on Running Stability of CRH3 High Speed Trains Passing by Each Other. *Engineering Applications of Computational Fluid Mechanics*, 8, 140-157.